Journal of Biomedical Optics

BiomedicalOptics.SPIEDigitalLibrary.org

Real-time absorption reduced surface fluorescence imaging

Bin Yang
James W. Tunnell

SPIE.

Real-time absorption reduced surface fluorescence imaging

Bin Yang and James W. Tunnell*
University of Texas at Austin, Department of Biomedical Engineering, Biophotonics Laboratory, Austin, Texas 78712, United States

Abstract. We introduce a technique that limits absorption effects in fluorescence imaging and does not require extensive imaging processing, thus allowing for video rate imaging. The absorption minimization is achieved using spatial frequency domain imaging at a single high spatial frequency with standard three-phase demodulation. At a spatial frequency $f = 0.5$ mm^{-1}, we demonstrated in both *in-vitro* phantoms and *ex-vivo* tissue that the absorption can be significantly reduced. In the real-time implementation, we achieved a video rate of 19 frames/s. This technique has potential in cancer visualization and tumor margin detection. [DOI: 10.1117/1.JBO.19.9.090505]

Keywords: fluorescence image; absorption reduction; spatial frequency domain imaging; high spatial frequency.

Paper 140409LRR received Jun. 26, 2014; revised manuscript received Sep. 4, 2014; accepted for publication Sep. 5, 2014; published online Sep. 24, 2014.

Fluorescence imaging of tissues is currently used in a number of clinical applications, including identification of epithelia cancers, localization of solid tumors, and the resection of lymph nodes.[1] Autofluorescence imaging highlights the biochemical properties of surface epithelial cancers for visualization and noninvasive diagnosis.[2–4] Furthermore, fluorescence imaging in conjunction with tumor targeting fluorescent probes may facilitate the delineation of tumor margins on excised tissues leading to complete resection and a lower local recurrence rate.[5] One challenge in fluorescence imaging is tissue absorption and scattering, which distorts the fluorescence intensity. Several studies have demonstrated that the attenuation introduced by the tissue can be well compensated by using model-based corrections.[6,7] Although these corrections are robust, lengthy data acquisition and processing can limit their usefulness in real-time imaging. Recently, a real-time imaging technique with absorption correction was reported which corrects the absorption by normalizing the fluorescence image to a reflectance image at the excitation wavelength using two cameras.[8] Here, we report an absorption reduced surface fluorescence imaging (ARSFi) technique using spatial frequency domain imaging (SFDI)[9] that allows for real-time image rendering. We implemented SFDI at a high spatial frequency to physically limit the imaging depth, thus reducing the absorption effects. We show that minimal computational processing is needed to render an ARSFi image, thus leading to a fast imaging speed of up to 19 frames/s using only one camera.

To reduce the tissue absorption in fluorescence imaging, we chose to limit the imaging depth by using SFDI imaging at a high spatial frequency. SFDI was first introduced for the quantitative evaluation of optical properties of a turbid medium using structured illumination.[9] SFDI has a spatial frequency-dependent sensitivity on both absorption and scattering.[10] At a high spatial frequency, SFDI has high sensitivity to scattering but low sensitivity to absorption. In a scattering dominant medium, the effective penetration depth δ'_{eff} can be described as

$$\delta'_{\text{eff}} = \left[\sqrt{3\mu_a(\mu_a + \mu'_s) + (2\pi f)^2}\right]^{-1}, \quad (1)$$

where μ_a and μ'_s are the absorption coefficient and the reduced scattering coefficient, respectively, and f is the spatial frequency. At a high spatial frequency, the penetration depth is mainly determined by the spatial frequency. Thus, Eq. (1) can be reduced to

$$\delta'_{\text{eff}} = (2\pi f)^{-1}. \quad (2)$$

Using high spatial frequency structured illumination, the imaging depth can be limited which results in reduced absorption in fluorescence imaging.

We obtained an absorption reduced fluorescence image by performing standard SFDI imaging and demodulating the fluorescence images at a high spatial frequency. Three patterns with phase shifts of 0, 120, and 240 deg were projected to the sample, and the corresponding fluorescence images I_1, I_2, and I_3 were recorded. The DC (planar) and AC (spatially modulated) images were obtained from the demodulation shown in

$$I_{\text{dc}} = 1/3(I_1 + I_2 + I_3), \quad (3)$$

$$I_{\text{ac}} = \sqrt{2}/3\left[\sqrt{(I_1 - I_2)^2 + (I_2 - I_3)^2 + (I_3 - I_1)^2}\right]. \quad (4)$$

The DC image would be the same as if the sample was illuminated by a planar excitation. On the other hand, the AC image is spatial frequency dependent and is also considered as the absorption reduced fluorescence image.

We developed a custom video rate SFDI fluorescence imaging system to perform real-time fluorescence visualization with absorption minimization. The LightCrafter evaluation module (LC-EVO, Texas Instruments, Dallas, Texas) was used to generate and project patterns. Specifically, the LC-EVO worked in a stored-pattern-sequence mode, which avoided the internal gamma correction. A noncooled CCD camera (piA2400-17 gm/gc, Basler, Ahrensburg, Germany) with a fast lens (Fujinon, Valhalla, New York, HF25HA-1B) was used for image acquisition. A 490 nm LED low-pass filtered at 500 nm was used for the excitation. A 510 nm high-pass filter (BrightLine FF510, Semrock, Rochester, New York) was used for fluorescence collection. The light engine of the LC-EVO was custom modified, thus the minimal diagonal image size was reduced from 25.4 to 2.8 cm with a 2 cm working distance to achieve high intensity illumination and high spatial frequency pattern. The projection magnification and working

*Address all correspondence to: James W. Tunnell, E-mail: jtunnell@mail.utexas.edu

distance can be adjusted to meet specific application requirements. In our study, the imaging area was 2.6 cm × 1.6 cm.

To study the spatial frequency-dependent performance of ARSFi, we imaged five tissue mimicking liquid phantoms at four spatial frequencies of 0.5, 0.35, 0.2, and 0.1 mm^{-1}. The phantoms were fabricated with a constant reduced scattering coefficient of $\mu_s' = 2.0\ mm^{-1}$ and a constant fluorescein concentration at 15 $\mu g/ml$, while the absorption increased from 0.05 to 0.45 mm^{-1} with an increment of 0.1 mm^{-1}. The results shown in Fig. 1 suggest that DC fluorescence experienced an approximately 70% drop in intensity at the highest absorption. On the other hand, the demodulated AC components were less affected by absorption at all spatial frequencies. Moreover, the absorption minimization performed better at a higher spatial frequency.

In the *ex vivo* tissue study, minced turkey breast was homogeneously mixed with fluorescein solution of a concentration of 0.18 mg/ml. Half of the tissue was further mixed with black India ink with $\mu_a = 0.42\ mm^{-1}$ to introduce additional absorption [Fig. 2(a)]. The tissue sample was imaged at a spatial frequency of 0.5 mm^{-1}. The raw fluorescence image showed the tissue with ink had a much lower intensity than the tissue without ink in Fig. 2(b). The ARSFi image [Fig. 2(c)] showed a more uniform intensity distribution over the entire tissue. The cross-sectional plot [Fig. 2(d)] suggested that the ink was responsible for an approximately 50% intensity drop in the raw fluorescence image, while only around a 10% drop in the AC image. Furthermore, in the AC image, an enhanced resolution and contrast can also be observed. This spatial frequency-based enhancement is consistent with the previous reports for both fluorescence and nonfluorescence imaging.[11,12] It needs to be noted that the dark zones in Fig. 2(c) suggest less fluorophore was distributed in those surface regions, which does not necessarily mean the absence of fluorophore located beneath the dark regions.

Although a good absorption minimization can be achieved, ARSFi is a surface fluorescence imaging technique. We conducted a depth analysis to show the depth-dependent properties of ARSFi. A fluorescent phantom with $\mu_a = 0.05\ mm^{-1}$ and $\mu_s' = 2\ mm^{-1}$ was embedded in a media with $\mu_a = 0.15\ mm^{-1}$ and $\mu_s' = 1\ mm^{-1}$. The phantom had a fluorescein concentration of 15 $\mu g/ml$. The phantom was gradually translated from the surface to 300 μm into the media with a step size of 50 μm. At the each depth, the phantom was imaged

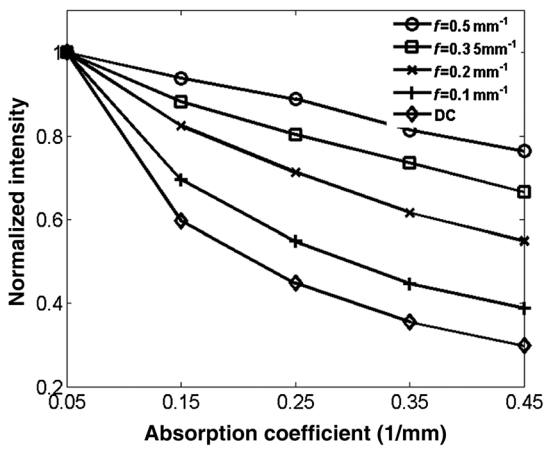

Fig. 1 Normalized fluorescence intensity of DC and AC components retrieved from five tissue mimicking phantoms with absorption increasing from 0.05 to 0.45 mm^{-1}.

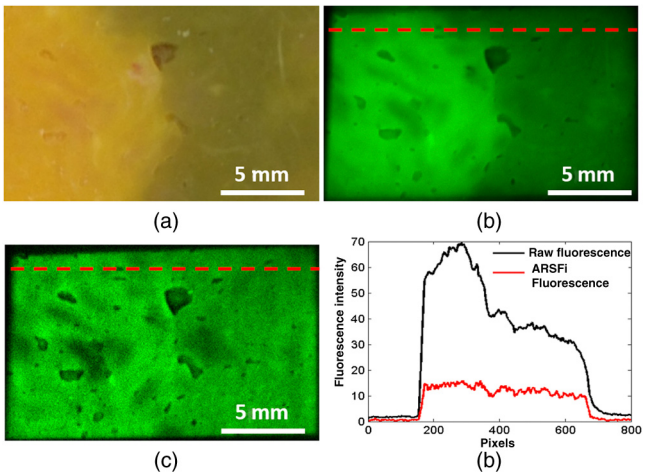

Fig. 2 Color image of *ex vivo* tissue model (a), raw fluorescence image (b), high spatial frequency fluorescence (c), and cross-sectional plot (d).

at $f = 0.5\ mm^{-1}$. The result (Fig. 3) shows that AC signal dropped rapidly as the phantom went deeper into the media. The fluorescence was marginally detectable when the sample was embedded ~300 μm into the media, which is close to the 330 μm imaging depth suggested by Eq. (2). This technique may not be suitable for certain image-guided surgery applications where the targeted tumor is deeply embedded in the tissue. Furthermore, while this study addresses the imaging system, we note that image-guided surgery is a multifaceted problem dependent as well on the fluorescent contrast agent development, delivery, and visualization. However, such a technique would be suitable for surface imaging applications such as tumor margin detection and epithelial tumor imaging.

The challenge of achieving real-time imaging with SFDI is that the standard SFDI demodulation technique requires three frames of the reflectance image, which is generally slow and is a source of motion artifacts. More advanced demodulation techniques require fewer frames, however, the image quality is compromised and requires more computational power.[13,14] To address this challenge, we optimized both image acquisition and image processing. To achieve a fast image acquisition, we used a highly efficient fluorescence collection system. We used an imaging camera having over 60% quantum efficiency at the emission wavelength with a fast lens having an $F/1.4$ large aperture. The fluorescence filter we used has over 93% transmission for the wavelengths longer than 515 nm. Together,

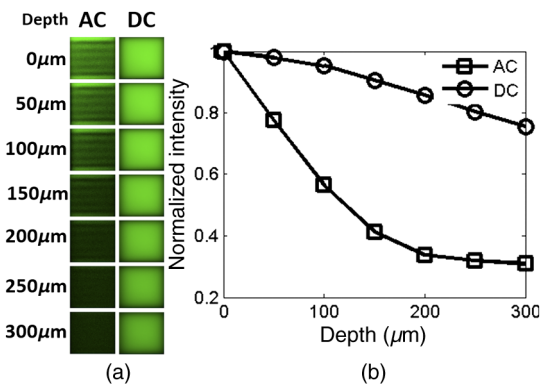

Fig. 3 (a) AC and DC fluorescence intensity at 7 depths. (b) Normalized AC and DC intensity plot at 7 depths.

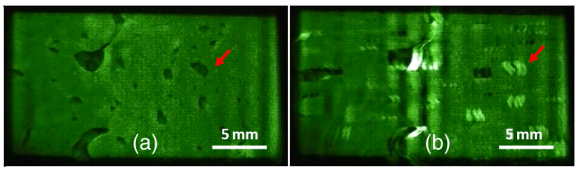

Fig. 4 Demodulated fluorescence image without motion (a) and with motion (b) (Video 1). The red arrow indicates the demodulated feature. With the motion, the ghost image can be observed (Video 1, MOV, 19.4 MB) [URL: http://dx.doi.org/10.1117/1.JBO.19.9.090505.1].

we were able to achieve good SNR images with a 20 ms integration time. To optimize the imaging processing, we adopted the following strategies: (1) utilize the cyclic projected patterns and (2) implement parallel threads and a 3-frame shared buffer for image acquisition and processing. Because the patterns are cyclic, starting from the third frame, for every newly acquired frame plus two previously acquired frames, we can derive a processed image, which is equivalent to conventional video-rate imaging, except the processed image has the "three-frame-motion-memory." We introduced parallel threads and a three-frame shared buffer to avoid asynchronization and competition between image acquisition and processing. The newly acquired image was pushed into the buffer and the oldest image in the buffer was then discarded. With the shared buffer, both image acquisition and image processing threads can be individually optimized without introducing interference between the two. Comparing this correction technique with model-based techniques, the advantage is evident as this technique only requires one incremental frame to derive one absorption reduced image versus nine frames for each attenuation corrected image using the model-based correction.

The real-time ARSFi system is able to perform raw image acquisition at 20 frames/s. The demodulated image can be displayed at around 19 frames/s (Video 1). Although the exposure was only 20 ms, the image read-out time currently limited the frame rate of the image acquisition. The motion memory in the current imaging system is around 150 ms, which means that the demodulated image is a temporal average over a 150-ms time period. It further suggests that 150 ms after the motion stops, the demodulated image will become stable. The typical motion artifact in real-time ARSFi is shown in Fig. 4. Without the motion, the demodulated image Fig. 4(a) faithfully represents the imaging field. In the presence of the motion, a ghost image can be observed in Fig. 4(b). The faster the motion, the more significant the motion artifact. The motion artifacts can be greatly reduced with a fast video camera.

In this letter, we presented a novel approach to reduce the absorption effects in fluorescence imaging by using SFDI at a high spatial frequency. Although the real-time ARSFi technique is not as robust as other model-based techniques, it provides the ability for video rate imaging. The real-time implementation of ARSFi suggests that this technique has potential in tumor margin detection and cancer visualization.

Acknowledgments

This research work was supported by grants from National Institutes of Health under Grants No. R21EB015892.

References

1. G. A. Wagnieres, W. M. Star, and B. C. Wilson, "In vivo fluorescence spectroscopy and imaging for oncological applications," *Photochem. Photobiol.* **68**(5), 603–632 (1998).
2. C. F. Poh et al., "Fluorescence visualization detection of field alterations in tumor margins of oral cancer patients," *Clin. Cancer Res.* **12**(22), 6716–6722 (2006).
3. N. Thekkek and R. Richards-Kortum, "Optical imaging for cervical cancer detection: solutions for a continuing global problem," *Nat. Rev. Cancer* **8**(9), 725–731 (2008).
4. B. Stenquist et al., "Bispectral fluorescence imaging of aggressive basal cell carcinoma combined with histopathological mapping: a preliminary study indicating a possible adjunct to Mohs micrographic surgery," *Br. J. Dermatol.* **154**(2), 305–309 (2006).
5. R. G. Pleijhuis et al., "Obtaining adequate surgical margins in breast-conserving therapy for patients with early-stage breast cancer: current modalities and future directions," *Ann. Surg. Oncol.* **16**(10), 2717–2730 (2009).
6. R. B. Saager et al., "Quantitative fluorescence imaging of protoporphyrin IX through determination of tissue optical properties in the spatial frequency domain," *J. Biomed. Opt.* **16**(12), 126013 (2011).
7. B. Yang, M. Sharma, and J. W. Tunnell, "Attenuation-corrected fluorescence extraction for image-guided surgery in spatial frequency domain," *J. Biomed. Opt.* **18**(8), 080503 (2013).
8. G. Themelis et al., "Real-time intraoperative fluorescence imaging system using light-absorption correction," *J. Biomed. Opt.* **14**(6), 064012 (2009).
9. D. J. Cuccia et al., "Modulated imaging: quantitative analysis and tomography of turbid media in the spatial-frequency domain," *Opt. Lett.* **30**(11), 1354–1356 (2005).
10. D. J. Cuccia et al., "Quantitation and mapping of tissue optical properties using modulated imaging," *J. Biomed. Opt.* **14**(2), 024012 (2009).
11. Mazhar Amaan et al., "Structured illumination enhances resolution and contrast in thick tissue fluorescence imaging," *J. Biomed. Opt.* **15**(1), 010506 (2010).
12. V. Krishnaswamy et al., "Structured light scatteroscopy," *J. Biomed. Opt.* **19**(7), 070504 (2014).
13. J. Vervandier and S. Gioux, "Single snapshot imaging of optical properties," *Biomed. Opt. Express* **4**(12), 2938–2944 (2013).
14. K. P. Nadeau, A. J. Durkin, and B. J. Tromberg, "Advanced demodulation technique for the extraction of tissue optical properties and structural orientation contrast in the spatial frequency domain," *J. Biomed. Opt.* **19**(5), 056013 (2014).